Speth et al. Functional Composite Materials (2023) 4:8
https://doi.org/10.1186/s42252-023-00045-z

Functional Composite Materials

RESEARCH Open Access

Study on mixing behaviour of aluminium-ceramic powder having high SiC volume fractions up to 50 vol.%

Marco Speth[1*], Kim Rouven Riedmueller[1] and Mathias Liewald[1]

Abstract

Aluminium matrix composites (AMC) do combine a high lightweight potential with a wide range of specific mechanical or thermal properties, depending on their material composition or the content of reinforcement particles, respectively. Currently, the three main production technologies for manufacturing such AMC are powder metallurgy, semi-solid processes and casting. Here, the AMC´s reinforcement proportion that can be processed depends on the chosen manufacturing strategy and is therefore often limited to a maximum value of 30 vol. %, due to agglomeration and porosity problems. In this context, the main objective is to understand the fundamental mixing behaviour of powder mixtures for AMC green body production having reinforcement contents of up to 50 vol.% SiC_p. For this purpose, powder mixtures of monomodal AlSi7Mg0.6 and different SiC_p fractions were prepared with different mixing times and speeds to investigate the influence of these mixing parameters on the homogeneity of the particle distribution. Afterwards, the influence of powder size on the mixing process was investigated. The results showed that a slower mixing speed resulted in faster homogenisation as well as a larger particle size can be faster mixed. Furthermore, a regression model was developed using mixing time, speed and particle loading, to determine sufficient mixing parameters.

Keywords Aluminium matrix composites (AMC), Al-SiC, Powder mixing, High particle loading, Coefficient of Variance (COV)

Introduction

Due to rising energy and material costs as well as environmental constraints to reduce carbon footprints of products, lightweight constructions have become indispensable in automotive, aviation or mechanical engineering. To meet those high demands on lightweight constructions, such as low weight and high strength [1] at the same time as well as wear resistance [2], respective components are frequently produced from composite materials. In particular, aluminium matrix composites (AMC), where ceramic particles are used to reinforce lightweight aluminium alloy components, show high lightweight potential in this context. Depending on the size, morphology and quantity of reinforcement particles, various specific properties can be achieved with such AMC without significantly increasing the low density of the aluminium alloy. Especially highly particle reinforced components over 30 vol.% can be used to improve thermal conductivity and reduce thermal expansion of the aluminium alloy. When manufacturing AMC, particular attention must be paid to ensuring homogenous distribution of the reinforcement particles within the component´s volume. These distributions tremendously influence the properties of such components, but, in the worst case, can lead to component failure due to inhomogeneous material characteristics. Depending on the amount of reinforcement particles, compared to the volume fraction of matrix

*Correspondence:
Marco Speth
marco.speth@ifu.uni-stuttgart.de
[1] Institute for Metal Forming Technology, University of Stuttgart, Stuttgart, Germany

aluminium alloy, mechanical, tribological as well as thermal properties can be modified according to given specifications. However, components with homogenous particle loadings beyond 30 vol.% SiC_p cannot be adequately met by currently known manufacturing processes due to high risk of agglomerations [3], porosity or inhomogeneous particle distributions [4]. Particle distributions in general are highly influenced by the process route used, while commonly AMC components are produced by casting (e.g. [5]), powder metallurgy (e.g. [6].) or semi-solid process routes (e.g. [7–9]). Three process routes in order to produce semi-finished products with higher particle loadings are friction stir processing (FSP), accumulative roll bonding (ARB) and nitridation-induced self-formed aluminium composite (NISFAC process). For FSP, components with up to 40 vol. % can be manufactured using a grooved base metal, which is bonded through friction stir welding [10]. ARB process uses aluminium sheet metal layers with particles in between, which are homogenously distributed inside the rolled components [11]. In NISFAC aluminium alloy powder is mixed with the reinforcement and subsequently heated and hold under nitrogen atmosphere, to produce components with up to 70 vol.% [12]. While all three processes show a sufficient process route to produce highly reinforced AMC, the manufacturing of complex shaped components without machining can be difficult.

Currently, at the Institute for Metal Forming Technology (IFU, Stuttgart) a novel process route, combining powder pressing and subsequent thixoforming, is investigated to produce high particle loadings up to 50 vol. % SiC_p. In order to obtain excellent material properties a homogenous distribution of the reinforcement particles is required prior processing. Therefore, in this regard several approaches can be found in literature. For example, mixing analysis of grinding wheel production processes is crucial for the grinding wheel quality. Therefore, a statistical distance-based mixing criterion based on the comparison of the mixture compared to the ideal homogeneous and inhomogeneous mixture was developed by Denkena et al. [13]. Another common approach is based on using the coefficient-of-variance of the mean near-neighbour distance of particles (COV_d) to characterize the homogeneity of AMC [14]. Yang et. al have thereby shown that the COV_d is insensitive to particle size, shape and particle loading, while showing high sensitivity to particle clustering [14]. The COV_d can be described by the following equation:

$$COV_d = \frac{\sigma_d}{d} \tag{1}$$

In order to determine the COV_d an image analysis of the microstructure based on the finite body tessellation is created according to Boselli et. al. [15]. The near neighbour distance is then defined as the shortest edge-to-edge distance between neighbouring particles that share a cell wall in the tessellated image. The resulting COV_d value (Eq. 1), which equals the standard deviation σ_d of the mean near neighbour distance divided by the average mean neighbour distance d, thereby indicates the homogeneity of the AMC.

While several studies can be found on the consolidation of powder mixtures for AMC as well as on the final manufacturing of AMC components, initial mixing of aluminium alloy powder with SiC_p is mainly performed on the basis of empirical values. Here, mixing times vary in most publications between 4 min [6] and 30 min [16] and a wide range of mixing speeds is used. The mixing results are then validated as homogenous without further investigations on the influence of these mixing durations and speeds. In this paper, the influence of the mixing parameters on the mixing process as well as the particle size for different particle loadings onto the particle distribution will be investigated. Aim is to identify the influencing mixing parameters to produce homogenous particle distribution with an empirical regression model.

Materials and methods

For the experimental investigation of the mixing parameters influencing the homogeneity of powdermixtures, AlSi7Mg0.6 and SiC_p particles of size F60 (300 – 242 µm) and F220 (75—53 µm) with a particle size range according to FEPA for SiC_p and Table 1 for AlSi7Mg0.6 were used.

So, different powders disclosing the same size distribution were mixed in order to ensure mixture analyses eliminating side effects due to different particle sizes. Powder mixtures with three different reinforcement proportions, namely 30, 40 and 50 vol.% SiC_p, were prepared applying different mixing durations and speeds (see Fig. 1). For mixing, a turbula mixer delivered by Dr. Fritsch Company, Germany was used, which exhibits a three-dimensional movement of the mixing basket as a combination of rotation, translation and inversion according to the 'Schatz geometry theory'. To assess required homogeneity after the mixing procedure within the respective powder mixtures, particle distribution was subsequently evaluated in plane and height

Table 1 Dry sieving analysis for the AlSi7Mg0.6 powder provided by Ecka Granules particle size by dry sieving (DIN EN ISO 4497)

Siev size	> 63 µm	> 20 µm	< 20 µm
AlSi7Mg0.6 (F220)	0.3%	90.2%	9.5%
Siev size	> 400 µm	> 250 µm	< 250 µm
AlSi7Mg0.6 (F60)	0.1%	96.6%	3.3%

Mixing parameters

Vol-%. SiC [%]	30	40	50	
Mixing time [min[	1	5	15	30 (only F60)
Mixing speed [min^-1]	20	40 (only F60)	60	

Fig. 1 Mixing parameters and experimental setup for mixing AlSi7Mg0.6 + SiC_p powder

direction via the levelled specimen. For this, a control volume shown in Fig. 1 was successively filled after a defined fraction of 1/3, 2/3 and 3/3 was taken of the respective powder mixture subsequently levelled and the homogeneity of the exposed surface was analysed in each case.

The levelled specimens were investigated with a microscope Keyence–vhx5000 and images of the distributions were taken. Followed by an image preparation using the *opencv library* within python, enhancing edge contrast using a contrast limited adaptive histogram equalization (clahe) filter and subsequently converting into a binary image. The python tool at the end detects all contours in the binary image in order to compute the nearest distances Δd between particles. A finite body tessellation as shown in Fig. 2 was used to define near neighbours of all particles, resulting in the mean near neighbour distance as well as the standard deviation of the mean near neighbour distance of all mixtures.

Results and discussion

Figure 3 shows images of three different mixing stages of the experiments. In these mixing stages, the mixing time was varied while mixing speed (20 min^{-1}) as well as particle size (F60) were kept constant. For each image, aluminium and SiC_p particles were poured together and mixed, where after 1/3 of the weight of the mixture was filled and levelled into the container of the analysing setup. In doing so, the image of a composite powder after one minute mixing (Fig. 3a) shows an inhomogeneous particle distribution with large aluminium or SiC_p agglomerates as highlighted by red circles. A more homogenous mixture is achieved after a mixing duration of 5 min, but some agglomerates can still be found (Fig. 3b). Further increase of the mixing duration up to 15 min results in an even more homogenous mixture. Here, no larger agglomerates can be visually detected.

In order to describe the mixing behaviour of the powder mixture in the turbula mixer a brief introduction of the flow behaviour is provided. Hereby, the powder mixing system needs to be described in a simplified manner using the so-called Froude number (Fr), which is a dimensionless number correlating the ratio between the centrifugal force and the gravity force both acting in a rotary drum. Dependent on filling degree and the Froude number Mellmann [17] defined different flow regimes in those applications. For a filling degree of 0.1, as used in this work, those flow regimes range from

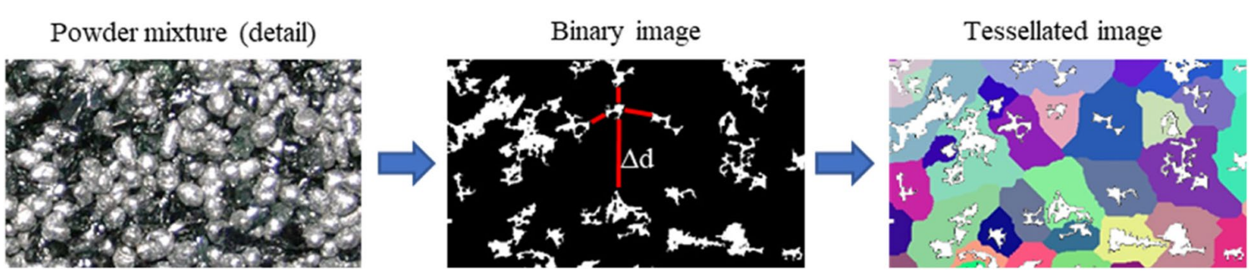

Fig. 2 Finite body tessellation in detail (Detailed image size)

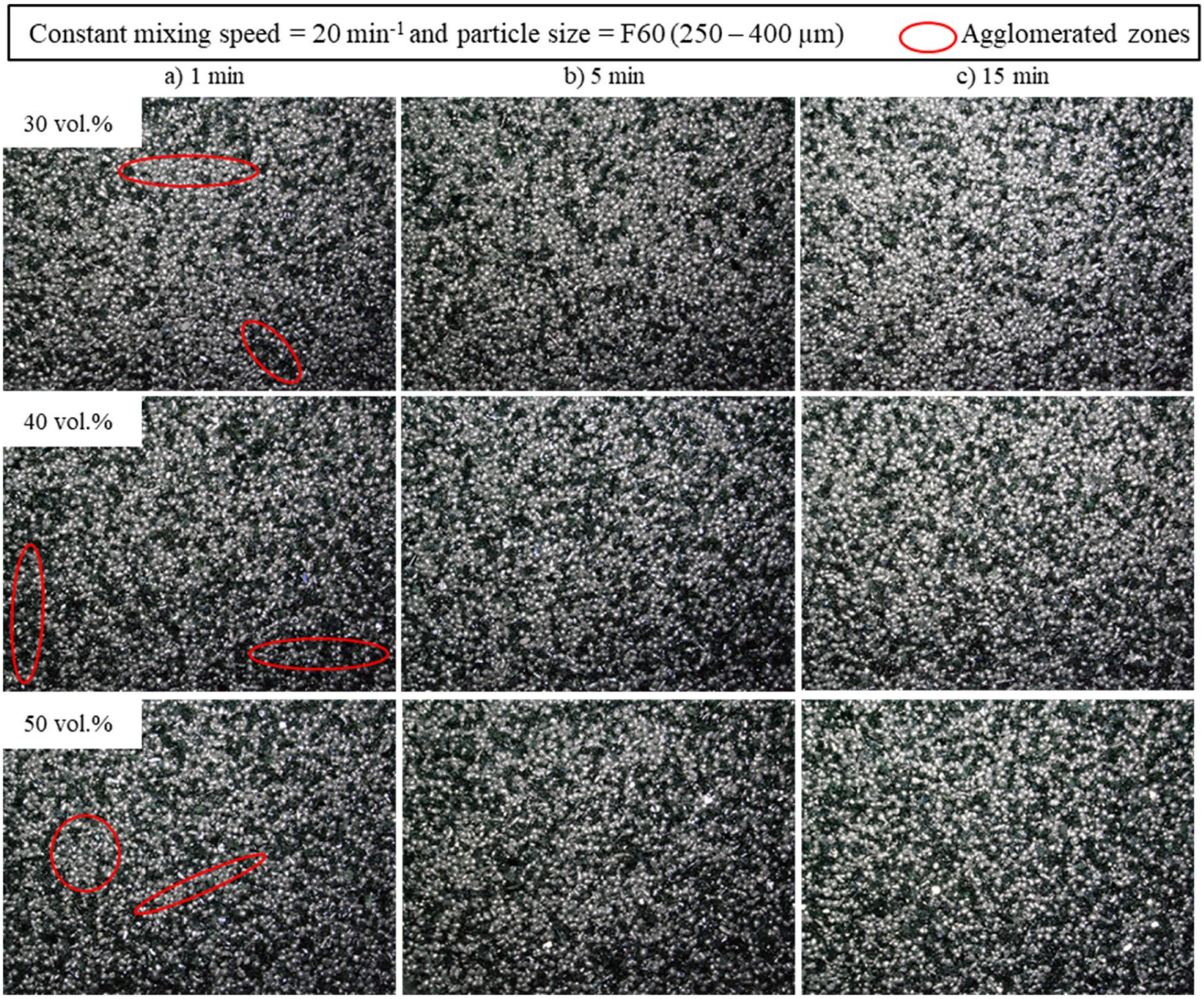

Fig. 3 Images of AlSi7Mg0.6 + 30 / 40 /50 vol.% SiC_p mixtures mixing with 20 min^{-1} after a) 1 min, b) 5 min and c) 15 min

slumping, rolling, cascading up to a cataracting flow behaviour of the powder (see Fig. 4a). According to Mayer-Laigle [18] the turbula mixer can be described with the Froude number dependent on motor speed, which equals Froude numbers of 0.2 (20 min^{-1}), 0.9 (40 min^{-1}) and 2.2 (60 min^{-1}) (see Fig. 4b). Therefore, a mixing speed of 20 min^{-1} is dominated from rolling and cascading powder movement, 40 min^{-1} shows a cascading, while 60 min^{-1} disclose a cataracting flow behaviour of particles. For cascading flow regimes at

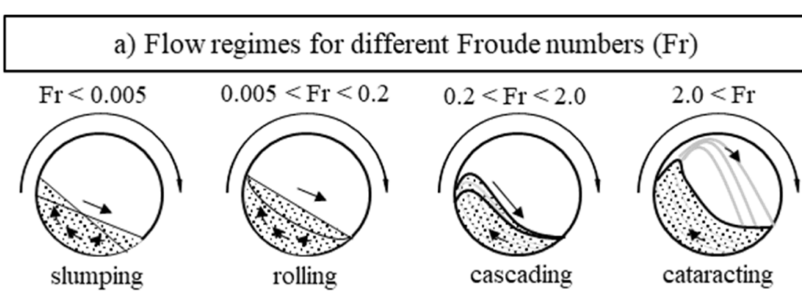

b) Fr for Turbula mixer

Mixing speed	Fr
20 min^{-1}	0.2
40 min^{-1}	0.9
60 min^{-1}	2.2

Fig. 4 **a** Flow regimes according to [17] and **b**) Froude numbers for Turbula mixers according to [18]

first mixing by convection occurs, due to the motion of particle clumps. Subsequently, the diffusion mixing, resulting from rearrangement of particles, as well as the shear mixing, due to velocity gradients between particle clumps, is dominant. In contrast to observed mixing mechanisms, free surface segregation appears in cascading flow regimes, powder flows in avalanches over the free surface and heavier or coarser particles will move further resulting in segregation. By increasing the mixing speed beyond the Froude number of the cascading flow regime, a higher centrifugal force acts on the particles resulting in a trajectory movement of single particles. In cataracting regimes, the prevailing mixing mechanism is convection and the contrary segregation mechanism is trajectory segregation, due to differences in projection emerging dependant on size and density of the particles. In general, the mixing quality is constantly changing for all flow regimes, due to the balancing of segregation and mixing effects. The pouring of the powder mixtures into the control volume exhibits a sliding behaviour for all samples, therefore this influence is ignored in this study.

Mixing results of the experiments, as depicted in Fig. 5, show the influence of mixing speed (x-axis) and mixing time (y-axis) onto the COV_d. The subplots show three different particle loadings for the samples mixed with F60 powder size, homogenous mixtures are achieved by passing the red dashed line.

For all particle loadings the mixing speed influences the reached homogeneity, in such a way that higher mixing speeds lead to a more inhomogeneous powder mixture. For 20 min^{-1} and 40 min^{-1} the main mixing mechanism was cascading, here the mixing was predominated by successive powder avalanches. In the beginning of the mixing process free surface segregation occurred, resulting in a slower mixing as speed increases to 40 min^{-1}, caused by the higher mass of the SiC_p and the associated increased momentum, which contributed to segregation. When applying even higher mixing speed of 60 min^{-1} the amount of centrifugal forces rises and can exceed the gravity forces, resulting in a cataracting flow behaviour of the powder. Hereby, the density difference of the powders increased segregation effects, while the SiC_p may still be in a cascading flow the lower density AlSi7Mg0.6 particles were starting to cataracting due to the lower inertial forces. In cataracting flows the trajectory segregation adds to the free surface segregation resulting in an additional segregation mechanism, which decreases the mixture homogeneity, compared to the other mixing speeds.

Mixing time finally shows a significant influence onto the homogeneity, independent of mixing speed and particle loading a mixing time of 15 min results in a

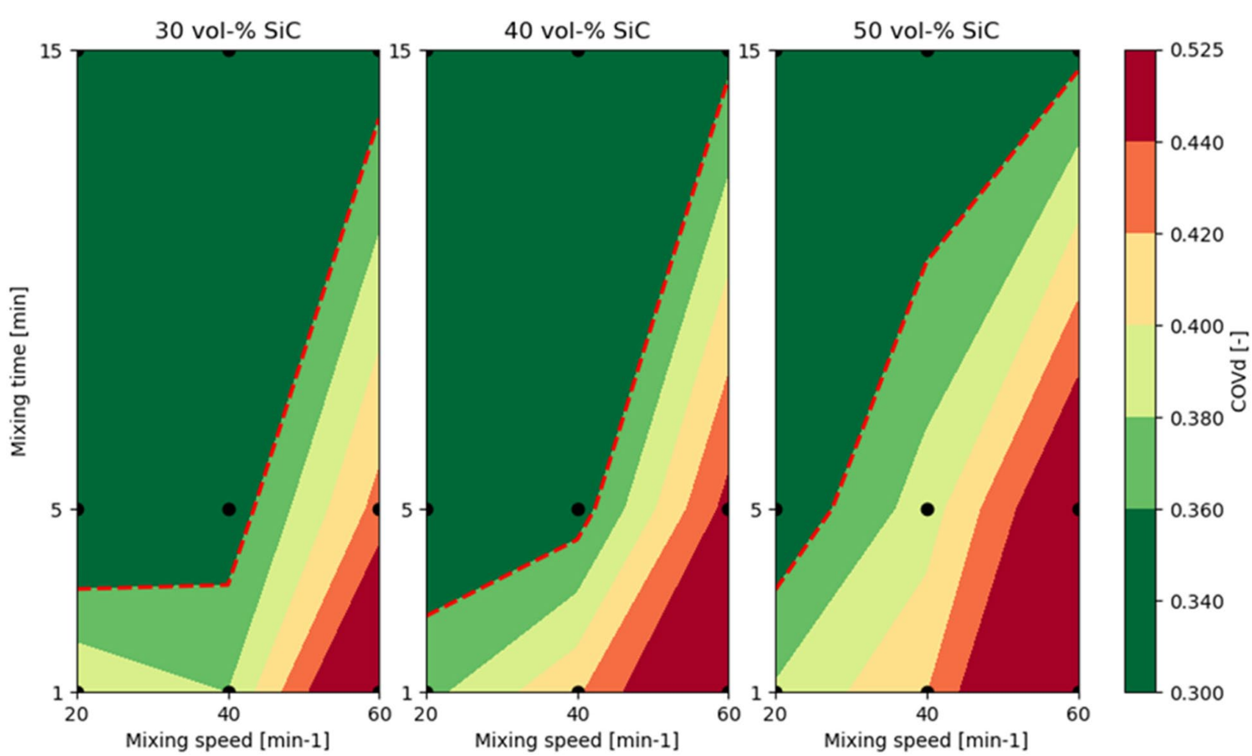

Fig. 5 Influence of mixing time and mixing speed onto the COVd depending on different particle loadings

homogenous mixture for all three powder combinations. The mixing mechanism are developing over mixing time resulting in a first macro mixing (powder avalanches) and subsequent diffusion (particle rearrangement) and shear mixing (due to different velocity gradients) of the powder. After a period of 15 min, however, further improvements in homogeneity were not observed anymore, so from production point of view a mixing time can be limited to 15 min in any case. For higher particle loadings longer mixing time is needed to reach a homogenous mixture, since the higher amount of SiC_p increased segregation effects (free surface and trajectory segregation).

The influence of powder size is shown in Fig. 6, hereby, in the first diagram the mixing speed was kept constant at 20 min^{-1} and in the second at 5 min. For smaller particle size (F220) the influence of mixing time was observed similar compared to the larger particle size (F60), but only an offset to higher COV_d values was noticed. The higher COV_d values resulted from the lower balance of segregation and mixing effects due to the smaller size of the powder, a more cohesive behaviour became apparent. While for the coarser powder (F60) a free surface flow was observed as dominant, the finer powder (F220) exhibits a more restricted motion of individual particles on the free surface due to the cohesive behaviour [19]. In the case of fine and cohesive powders, the convection mixing (motion of particle clumps) is reduced due to agglomeration of the finer powder, therefore a mixing through shearing is needed in order to separate larger agglomerates of AlSi7Mg0.6 und SiC_p respectively. The separation of both powders through shearing before cohesion mixing in fact results into a slower and higher COV_d value over mixing time. Since the free surface flow of the finer powder is limited, the influence of mixing speed shows a negligible effect onto the mixture homogeneity. Trajectory segregation due to higher mixing speeds weren´t observed in this context. Therefore, in contrast to the powder with larger grain size the mixing behaviour of the powder with smaller grain size is not influenced by mixing speeds up to 60 min^{-1}.

To determine the optimal mixing parameters for differing powder mixtures, a quadratic regression (Eq. 2) of the three main influencing parameters x_1 mixing time [min], x_2 mixing speed [min^{-1}] and x_3 particle loading [vol. %] was estimated. The regression coefficients of the different parameters are shown in Fig. 7, thereby a separation of the two powder sizes was performed in order to improve the predictability of the regression models. For a powder size above 100 µm up to 400 µm the coefficient of determination (r^2),

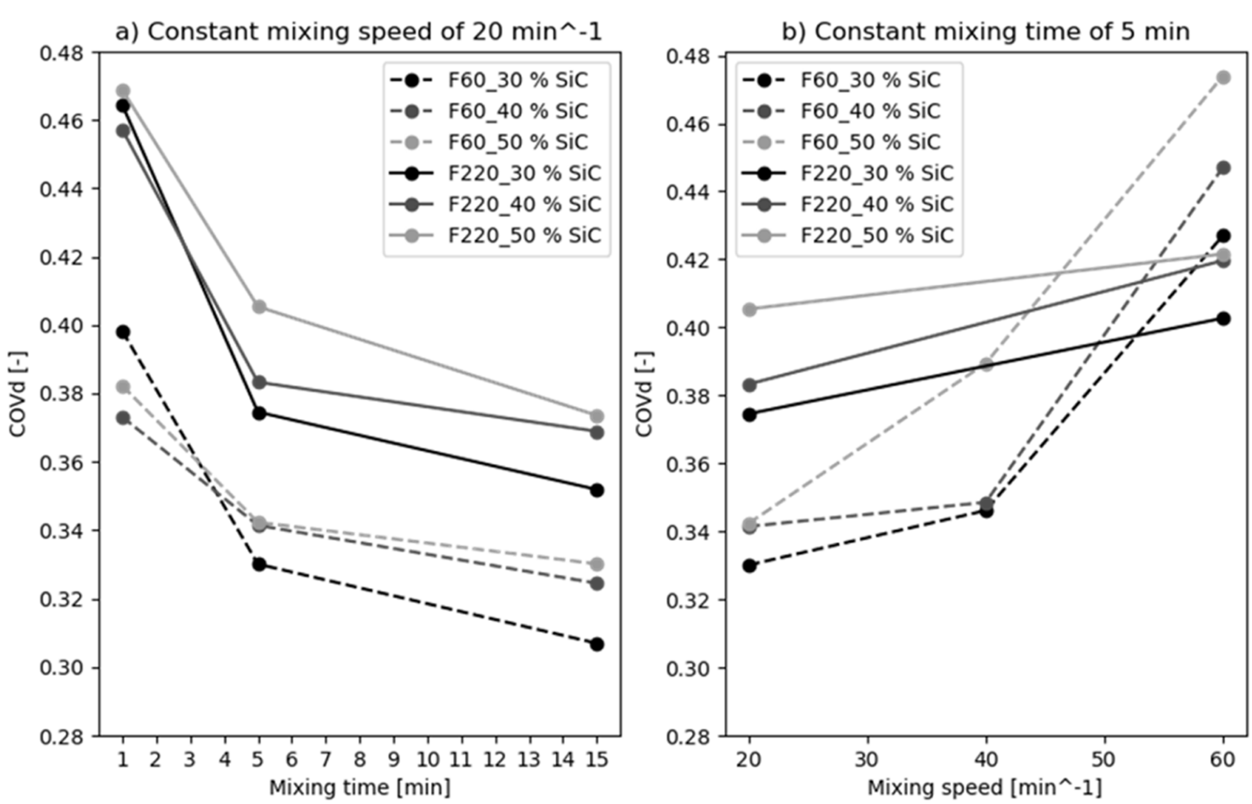

Fig. 6 Influence of powder size on mixing time and mixing speed

which characterizes the quality of predictions, was found to 0.94 and for powders having particle sizes below 100 µm and above 20 µm r^2 to 0.95, showing a good estimation quality. For the regression model the square term as well as the interaction terms of the particle loading parameter are dropped, as the curves are only shifted depending on the particle loading. So, the dependency of particle loading (coefficient m_3) onto the mixing result is lower compared to the main mixing parameters. The linear coefficient m_1 of the regression model shows the highest value of all coefficients for both models, which relates to the highest influence of mixing time onto the process as already discussed in the discussion before. For the higher grain size, the influence of mixing speed onto the result can be investigated by the higher m_2 value compared to the near zero value of the smaller grain size. Since the curves show a non-linear behaviour additionally quadratic input parameters (m_4 and m_5) were chosen resulting in a similar behaviour to the linear coefficients with a higher influence of the mixing speed. The correlation between mixing time and speed should also be considered, which is for larger grain sizes a bit higher compared to smaller grain sizes as seen by the coefficient m_6.

$$COV_d = m_1 * x_1 + m_2 * x_2 + m_3 * x_3 + m_4 * x_1^2 + m_5 * x_2^2 + m_6 * x_1 * x_2 \tag{2}$$

A comparison of the predicted curve to the experimental curve is shown in Fig. 7 a)-d), while for Fig. 7 a), c) a constant mixing speed of 20 min^{-1} and Fig. 7 b), d) a constant mixing time of 5 min is displayed. All diagrams show a good match between the experimental curves and the predicted, although some minor deviation can be investigated. In each experimental result a deviation due to the influence of a small randomness in particle size distribution was noticed, which couldn´t be fit by a regression line. The size influence for larger particles (> 400 µm) and smaller particles (< 20 µm) will be a limit to the regression model, since the behaviour especially for the smaller powder changes due to the particle interaction and friction in the powder. Another limit to the regression model is the scalability for larger weights of powders above the volume of this turbula mixer (2 l), as well as a differing mixing motion. The regression model can only be used for dry powder mixing. However, for future work with similar powders a mixture homogeneity can be predicted by those diagrams. Thus, the homogenous mixture of AlSi7Mg0.6 powder with different amounts SiC_p can be ensured without any further experimental effort.

Conclusion

Aim of this research is the production of AMC components with high particle loadings, which can currently not be manufactured by conventional processes, by combining powder pressing with subsequent semi-solid forming. In order to meet specific material properties a homogenous particle distribution must be guaranteed. Therefore, this paper focused on mixing characteristics of AMC powder mixtures with high SiC_p contents of up to 50 vol.%. First, powder mixtures with a particle size range of F60 and different particle loadings (30, 40, 50 vol.%) were mixed at varying mixing speeds and times to determine the influence of these process parameters on the homogeneity of particle distribution. The particle distribution was subsequently detected by an optical measurement system and analysed using finite body tessellation. The following results were found:

- Mixing in the cascading flow behaviour of the powder mixture (20 min^{-1}, 40 min^{--1}) showed a homogenous mixture after 5 min of mixing, due to the mixing through avalanches on the free surface. Segregation resulted only from density differences of both powders.
- A higher mixing speed of 60 min^{-1} increased the resulting mixing time up to 15 min in order to produce a homogenous mixture, caused by the increasing centrifugal forces, adding trajectory segregation along with the free surface segregation.
- A mixing speed below a Froude number of 2 (cascading flow behaviour) should be choosen for mixing of AMC powders in a turbula mixer.
- Independent of mixing speed, a mixing time of 15 min resulted in a homogenous particle distribution for all investigated particle loadings (30, 40, 50 vol.%). By increasing particle loading up to 50 vol.% an increased mixing time was needed in order to guarantee a quite homogenous mixture. As a result of the higher particle loading the amount of free surface segregation increased during mixing.
- During mixing a more cohesive behaviour of the smaller powder size (F220) with a limited free surface flow of such kind of powders was examined. Thus, resulting in a slower mixing behaviour in general, first larger particle clumps need to be sheared or separated to smaller agglomerates in order to achieve a homogenously mixed powder.

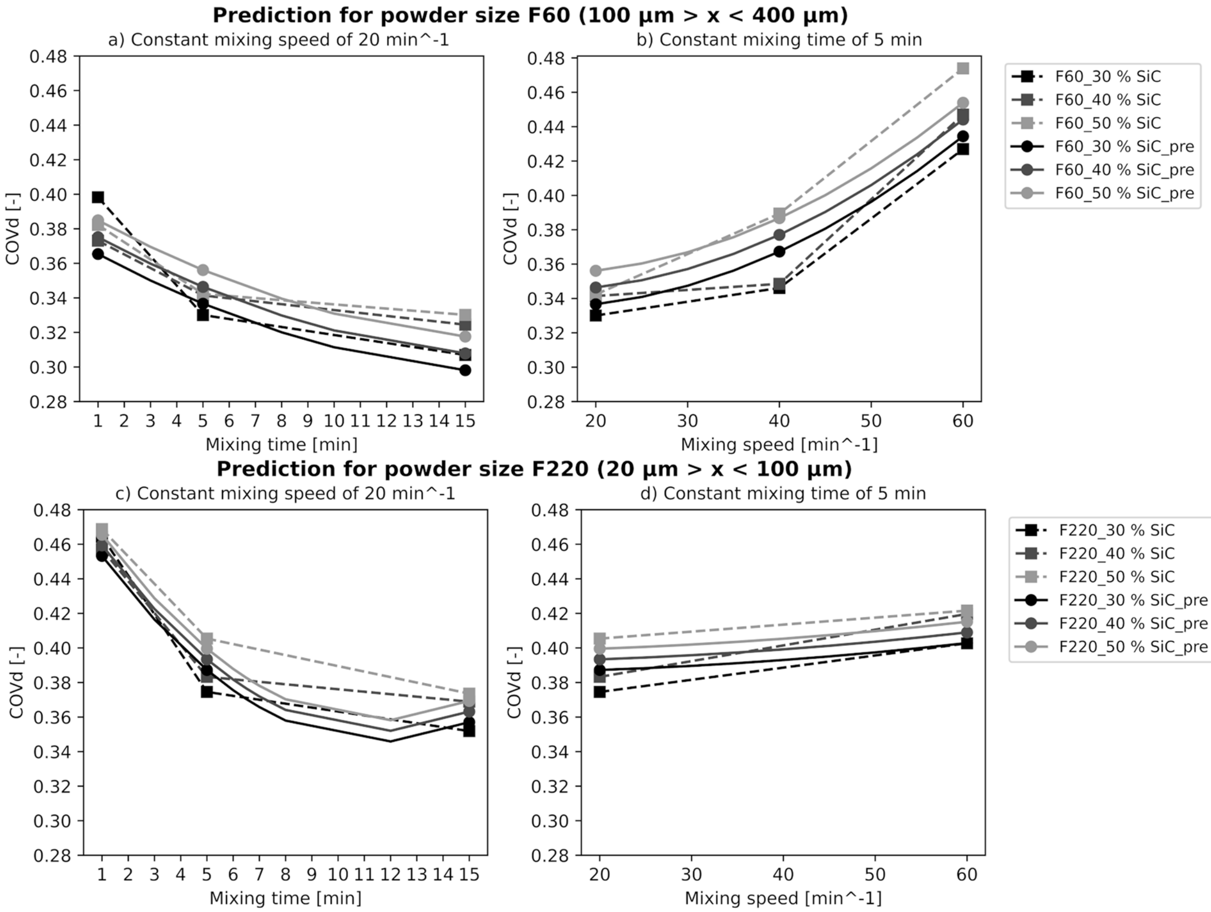

Particle size	m_1	m_2	m_3	m_4	m_5	m_6
100 µm - 400 µm	-6.61432e-03	-7.01997e-04	9.74234e-04	2.38248e-04	4.55903e-05	-1.00185e-04
20 µm - 100 µm	-2.22226e-02	6.27486e-08	6.15574e-04	9.62479e-04	5.01989e-06	-2.41899e-06

Fig. 7 Regression models for both powder sizes (F60 & F220) and coefficients used

- A regression model dependent on particle size was fitted, to determine mixing results for different particle loadings and mixing parameters. The model showed a good correlation overall and can be used for future research dealing with similar properties of AMC powders.

In future research the influence of powder pressing prior heating as well as subsequent semi-solid forming onto the particle distribution will be investigated.

Acknowledgements
The authors would like to thank Mr. Toni Kemter for helping in the preparation of the mixing experiments.

Authors' contributions
Marco Speth did the experiments and interpreted the results. Mathias Liewald and Kim Rouven Riedmueller assisted with the interpretation of the results and reviewed and rephrased the manuscript. Marco Speth wrote the main manuscript text and prepared the figures. All authors read and approved the manuscript.

Funding
Open Access funding enabled and organized by Projekt DEAL. The authors like to thank German Research Foundation (DFG) for their financial support of the research project (LI1556/72–1) "Manufacturing of application-specific components from particle reinforced aluminium matrix composites using a combination of powder pressing and thixoforging".

Availability of data and materials
The data presented in this study are available on request from the corresponding author.

Declarations

Competing interests
The authors have no conflicts of interest to declare that are relevant to the content of this article.

Received: 25 November 2022 Accepted: 28 May 2023
Published online: 08 June 2023

References

1. A. Bhowmik, D. Dey, A. Biswas, Microstructure, mechanical and wear behaviour of Al7075/SiC aluminium matrix composite fabricated by stir casting. Indian J. Eng. Mater. Sci **28**(01), 46–54 (2021)
2. D. Dey, A. Bhowmik, A. Biswas, Effect of SiC Content on Mechanical and Tribological Properties of Al2024-SiC Composites. SILICON **14**(1), 1–11 (2022)
3. G. O. Donnell, B. S. Eng and L. Looney, "Process Optimisation and Numerical Modelling of Powder Metallurgical Aluminium Matrix Composites", Dublin City University, 1999.
4. D.S.B. Heidary, F. Akhlaghi, Theoretical and experimental study on settling of SiC particles in composite slurries of aluminum A356/SiC. Acta Mater. **59**(11), 4556–4568 (2011)
5. G. Upadhyay, K.K. Saxena, Role of Stir Casting in development of Aluminium Metal Matrix Composite (AMC): An Overview. IOP Conf. Ser. Mater. Sci. Eng. **1116**(1), 012022 (2021)
6. G. O'Donnell, L. Looney, Production of aluminium matrix composite components using conventional PM technology. Mater. Sci. Eng. A **303**(1–2), 292–301 (2001)
7. A. Storz, T. Schubert, T. Weissgärber, C. Seyboldt, K.R. Riedmüller, Efficient Processing of Metal-Matrix-Composites by Combining Direct Pressure Sintering and Subsequent Thixoforging. Mater. Sci. Forum **825–826**, 167–175 (2015)
8. K. Riedmüller, M. Liewald and L. Kertesz, "Manufacturing of Composite and Hybrid Materials by Semi Solid Forming", in 12th International Conference on Semi-Solid Processing of Alloys and Composites S2P2012, 2012.
9. B.-A. Behrens, C. Frischkorn, Thixoforging of particle-reinforced steel materials. Prod. Eng. **8**(3), 335–343 (2014)
10. S. Rathee, S. Maheshwari, A.N. Siddiquee, M. Srivastava, Investigating Effects of Groove Dimensions on Microstructure and Mechanical Properties of AA6063/SiC Surface Composites Produced by Friction Stir Processing. Trans. Indian Inst. Met. **70**(3), 809–816 (2017)
11. M. Reihanian, E. Bagherpour, M.H. Paydar, On the achievement of uniform particle distribution in metal matrix composites fabricated by accumulative roll bonding. Mater. Lett. **91**, 59–62 (2013)
12. D.-Y. Kim, P.-R. Cha, H.-S. Nam, H.-J. Choi, K.-B. Lee, Effect of Material and Process Variables on Characteristics of Nitridation-Induced Self-Formed Aluminum Matrix Composites—Part 1: Effect of Reinforcement Volume Fraction, Size, and Processing Temperatures. Materials (Basel) **13**(6), 1309 (2020)
13. B. Denkena, A. Krödel, M. Kostka, F.L. Kempf, "Mischanalyse in der Schleifscheibenherstellung", *wt Werkstattstech*. Online **10**, 735–739 (2021)
14. N. Yang, J. Boselli, I. Sinclair, Simulation and quantitative assessment of homogeneous and inhomogeneous particle distributions in particulate metal matrix composites. J. Microsc. **201**(2), 189–200 (2001)
15. J. Boselli, P.D. Pitcher, P.J. Gregson, I. Sinclair, Secondary phase distribution analysis via finite body tessellation. J. Microsc. **195**(2), 104–112 (1999)
16. H.R. Hafizpour, A. Simchi, Investigation on compressibility of Al-SiC composite powders. Powder Metall. **51**(3), 217–223 (2008)
17. J. Mellmann, The transverse motion of solids in rotating cylinders-forms of motion and transition behavior. Powder Technol. **118**(3), 251–270 (2001)
18. C. Mayer-Laigle, C. Gatumel, H. Berthiaux, Mixing dynamics for easy flowing powders in a lab scale Turbula® mixer. Chem. Eng. Res. Des. **95**, 248–261 (2015)
19. R. Hogg, Mixing and Segregation in Powders: Evaluation, Mechanisms and Processes. KONA Powder Part. J. **27**(27), 3–17 (2009)

Publisher's Note